Seasonal and diurnal measurements of carbon monoxide and nonmethane hydrocarbons at Mt. Wilson, California: Indirect evidence of atomic Cl in the Los Angeles basin

Katrine A. Gorham [a,*], Nicola J. Blake [a,1], Richard A. VanCuren [b,2], Henry E. Fuelberg [c,3], Simone Meinardi [a,4], Donald R. Blake [a,5]

[a] Department of Chemistry, University of California, Irvine, CA 92697, USA
[b] California Air Resources Board, Sacramento, CA, 95814, USA
[c] Department of Meteorology, Florida State University, Tallahassee, FL 32306, USA

ABSTRACT

We present a study of the seasonal and diurnal variability of carbon monoxide and selected volatile organic compounds in the Los Angeles area. Measurements were made during four different nine-day field campaigns in April/May, September, and November, 2007, and February, 2008, at the Mt. Wilson sampling site, which is located at an elevation of approximately 1700 m in the San Gabriel Mountains overlooking Pasadena and the Los Angeles basin. The results were used to characterize the Mt. Wilson site as a representative location for monitoring integrated Los Angeles basin emissions, and, by reference to carbon monoxide emissions, to estimate average annual emissions. The considerable seasonal variability of many hydrocarbons, in both their measured mixing ratios and their relationship to carbon monoxide, was indicative of variable source strengths. Most interestingly, perturbation of C_4 hydrocarbon ratios suggested an enhanced role for chlorine chemistry during the month of September, likely as the result of Los Angeles' coastal location. Such coastal influence was confirmed by observations of enhanced mixing ratios of marine halocarbons, as well as air mass back trajectories.

© 2010 Elsevier Ltd. All rights reserved.

1. Introduction

Since the 1950s, the Los Angeles basin has been well known for its photochemically induced air pollution/urban smog and generally highly oxidizing environment (Haagen-Smit, 1952; Renzetti, 1956; Finlayson-Pitts and Pitts, 2000). Volatile organic compounds (VOCs) are emitted into the atmosphere as the result of many anthropogenic industrial and combustion processes, as well as from biogenic sources, and play an important role in a wide range of tropospheric chemical reactions, including ozone (O_3) production. Oxidation of VOCs, often in the form of nonmethane hydrocarbons (NMHCs), typically occurs via reaction with hydroxyl radicals (OH). When primary pollutants are oxidized and exposed to sunlight in the presence of nitrogen oxides ($NO_x = NO + NO_2$), the resulting reaction produces a variety of secondary pollutants including O_3,

$$VOC + NO_x + h\upsilon \rightarrow O_3 + \text{other products}$$
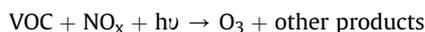
which contributes to urban smog and the detrimental health effects associated with urban air (Lippmann, 1991). In addition to OH, NMHC oxidation can also occur via reaction with other radicals including chlorine (Cl) atoms (Chameides et al., 1992; Finlayson-Pitts, 1993; Finlayson-Pitts and Pitts, 2000). Chlorine atoms are thought to be important oxidants in marine areas (Finlayson-Pitts, 1993), where marine air masses can be traced using halocarbon markers (e.g. Blake et al., 1996; Butler et al., 2007).

The earliest measurements of NMHCs in the Los Angeles basin date back to the 1960s, as reported by Gordon et al. (1968). Since then, there have been numerous other studies investigating atmospheric hydrocarbons in the city of Los Angeles and the Los Angeles basin (e.g. Levitt and Chock, 1976; Lonneman et al., 1974; Elkus and Wilson, 1977; Fraser et al., 1997; Chung et al., 2003; Croes and Fujita, 2003; Fujita et al., 2003; Qin et al., 2004; Brown et al., 2007; Baker et al., 2008). Several of these studies have focused on

* Corresponding author. Tel.: +1 303 349 2884.
E-mail addresses: katrine@polarfield.com (K.A. Gorham), nblake@uci.edu (N.J. Blake), rvancure@arb.ca.gov (R.A. VanCuren), fuelberg@met.fsu.edu (H.E. Fuelberg), smeinard@uci.edu (S. Meinardi), drblake@uci.edu (D.R. Blake).
[1] Tel.: +1 603 664 2916.
[2] Tel.: +1 916 327 1511.
[3] Tel.: +1 850 644 6466.
[4] Tel.: +1 949 824 3407.
[5] Tel.: +1 949 824 4195.

the weekend–weekday effect where VOC-limited ozone formation causes elevated levels of ozone to be observed on the weekend, preceded by elevated levels of ozone precursors during the week (Levitt and Chock, 1976; Elkus and Wilson, 1977; Fraser et al., 1997; Fujita et al., 2003; Qin et al., 2004). Other studies have focused on source identification or city comparisons (Brown et al., 2007; Baker et al., 2008). While air quality in the Los Angeles basin has improved, it is still designated as an ozone non-attainment area and exceeded national 8-h (0.075 ppm) and state 1-h (0.090 ppm) standards for ozone on 108 and 96 days, respectively, during 2007 (CARB, 2007a).

The work presented here investigates seasonal trends and influences on the NMHC composition of the Los Angeles basin with the goal of contributing to the development of more effective air pollution control strategies for this area. It is important to understand short-term variations so that control strategies can appropriately reflect the diurnal and seasonal differences in atmospheric chemistry and emissions, as well as establish baseline measurements to assess long-term trends associated with VOC emissions.

2. Methods

2.1. Sampling site

All samples were collected at the Mt. Wilson Observatory (34.22°N, 118.05°W) (Fig. 1), which is located at approximately 1700 m elevation, 26 km northeast of downtown Los Angeles, and approximately 53 km from the Port of Los Angeles in San Pedro, the United States' highest ship traffic port in 2007 (AAPA, 2008). The topography of the Los Angeles basin is unique because it is surrounded on three sides by mountains, and the Pacific Ocean to the west and southwest, which results in vertical circulation associated with a westerly sea breeze (Lu and Turco, 1995, 1996).

The Mt. Wilson site was chosen by the California Air Resources Board as part of a larger study to quantify time-varying concentrations of greenhouse gases and related hydrocarbon species at various sites in Southern California, with the goal of tracking the emissions and fluxes of these gases from the Southern California region.

2.2. Sampling

Hour-long integrated whole air samples were collected 24-h per day during four different nine-day periods between April 2007 and February 2008 at the Mt. Wilson Observatory (with a total of 216 canister samples collected for each sampling period). The nine-day

periods were selected in order to sample during two Saturday–Sunday periods and one Monday–Friday period. The four different sampling periods were April 28–May 6 (2007), September 8–September 16 (2007), November 10–November 18 (2007), and February 9–February 17 (2008). Ideally, sampling would have also been conducted during July/August, however, the dates were selected in accordance with availability of resources. Sampling was performed using a stainless steel single metal bellows pump (Model MB-302, Senior Aerospace Metal Bellows, Sharon, MA) connected to a ¼ inch stainless steel inlet located approximately 3.5 m above the ground. With the use of a mass flow controller (Brooks Instrument, Hatfield, PA), ambient air was pressurized in the canisters to approximately 30 psig. Samples were collected in electropolished 2 l stainless steel canisters, fitted with Swagelok Nupro metal bellows valves. Prior to sampling, each canister was pre-conditioned and flushed with ultra-high purity helium, and evacuated to 10^{-2} Torr.

2.3. Analysis

All whole air samples were analyzed at our University of California, Irvine, laboratory for a suite of 54 hydrocarbons, halocarbons, and alkyl nitrates by cryogenic preconcentration and split injection (2370 cm^3 at standard temperature and pressure) into a multicolumn/detector gas chromatography (GC) system, described in detail by Colman et al. (2001). This system employed the use of two flame ionization detectors (FID), two electron capture detectors (ECD), and one quadrupole mass spectrometer (MSD). Trace gases were quantified using five different column/detector combinations housed in three individual Hewlett–Packard ovens (Model HP-6890). The different column/detector combinations were as follows: J&W-DB-1/FID, J&W-PLOT+DB-1/FID, RESTEK-1701/ECD, J&W-DB-5+RESTEK-1701/ECD, and J&W-DB-5ms/MSD. Absolute accuracy is estimated to vary from 2 to 10%. The limit of detection is 3 pptv for nonmethane hydrocarbons, 0.03 pptv for alkyl nitrates, and less than 0.1 pptv for the halocarbons of interest. For the hydrocarbons of interest in this study the measurement precision is 1% or 1.5 pptv (whichever is larger) for the alkanes and alkynes, 3 pptv or 3% (whichever is larger) for the alkenes. The precision varies from 5 to 10% for alkyl nitrates and is 1–5% for the halocarbons of interest. The whole air samples were also analyzed for carbon monoxide (CO) using a separate GC system that employed a packed column separation followed by catalytic conversion of CO to CH$_4$ and subsequent detection by FID. The limit of detection for CO is 1 ppbv, with an accuracy of 5–7% and 4 ppbv precision.

2.4. Meteorological parameters

Meteorological measurements of wind speed gradients (Model 010C, Met One Instruments, Inc, Grants Pass, OR), wind direction (Model 020C, Met One Instruments), and temperature (Model 060-1, Met One Instruments) were made during each of the field seasons as part of the California Air Resources Board suite of continuous measurements. These measurements were averaged over 1 h time periods corresponding with the 1 h integrated whole air samples.

3. Results and discussion

3.1. Diurnal and seasonal trends

Carbon monoxide measured during all four sampling periods followed a very distinct diurnal trend, with daytime maxima in the early afternoon at 14:00 ± 2:00 (local time) and nighttime minima in the late evening or early morning at 02:00 ± 4:00 (local time) (Fig. 2 and Table 1). The hydrocarbons (Table 1) followed similar diurnal trends.
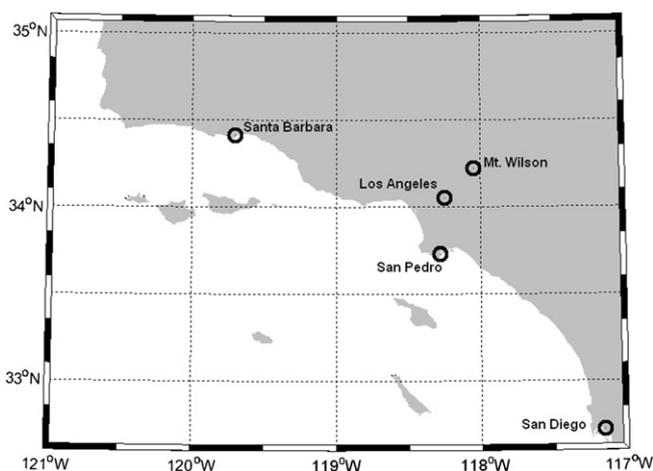

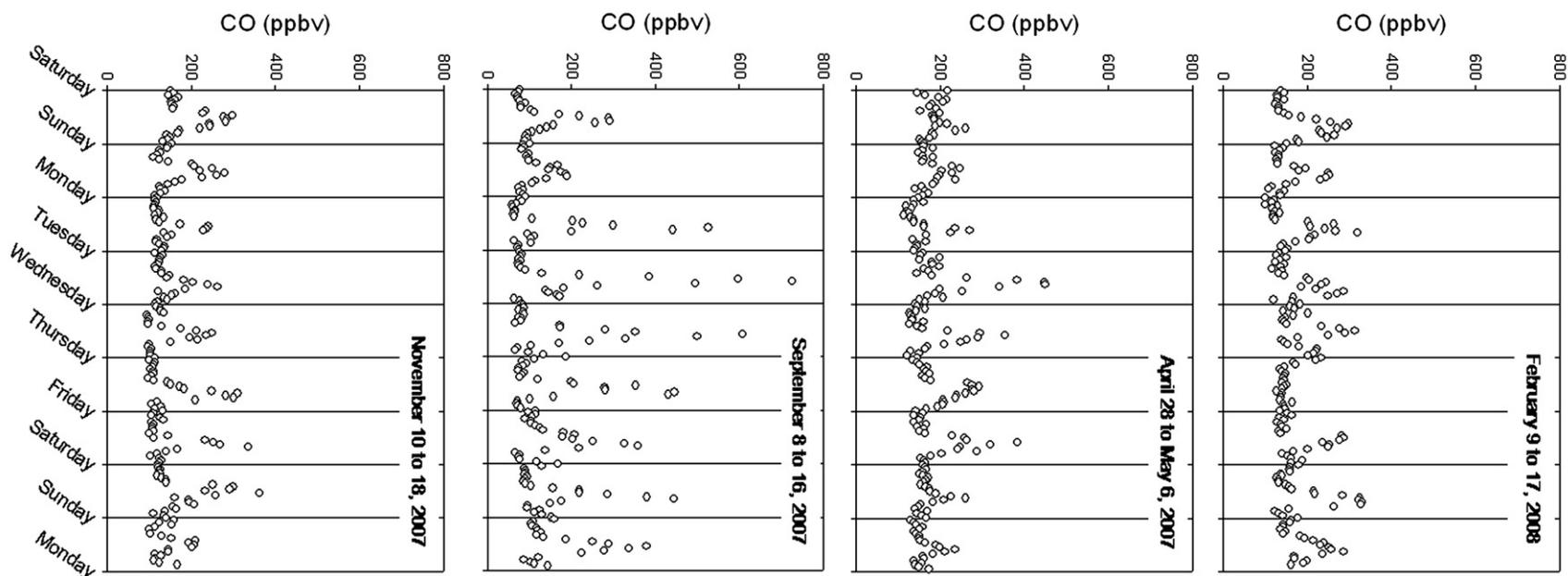Fig. 1. Map of the Southern California coast.

Fig. 2. Time series for CO during four different sampling periods. Each data point represents an hour-long integrated sample, with the initial sample collected Saturday, 00:00–01:00 local time.

Table 1
Diurnal maxima and minima during four different sampling periods. Reported values are mean daytime maxima and nighttime minima mixing ratios, with minimum and maximum displayed in parentheses. Quoted uncertainties are 1-sigma. ND indicates below limit of detection. Units are pptv unless otherwise stated.

Compound	February		April/May		September		November	
	Daytime maxima	Nighttime minima	Daytime maxima	Nighttime minima	Daytime maxima	Nighttime minima	Daytime maxima	Nighttime minima
CO (ppbv)	294 ± 25 (249, 329)	119 ± 10 (98, 133)	304 ± 73 (233, 447)	132 ± 13 (112, 149)	439 ± 163 (187, 725)	67 ± 11 (55, 91)	281 ± 49 (207, 361)	106 ± 16 (92, 144)
Ethane	3525 ± 978 (2531, 4919)	1358 ± 251 (1042, 1816)	3264 ± 943 (2273, 4616)	1250 ± 220 (842, 1544)	5363 ± 2512 (2159, 10,497)	400 ± 97 (318, 633)	2239 ± 600 (1538, 3237)	719 ± 171 (522, 943)
Propane	2731 ± 1160 (1508, 4628)	531 ± 242 (232, 930)	2313 ± 1235 (1173, 4365)	356 ± 148 (139, 631)	5138 ± 2420 (1313, 8766)	36 ± 25 (13, 95)	2116 ± 725 (1161, 3027)	219 ± 134 (85, 440)
i-Butane	693 ± 295 (425, 1264)	72 ± 41 (24, 135)	392 ± 211 (208, 763)	28 ± 13 (5, 45)	1144 ± 589 (359, 2291)	ND (ND, 4)	343 ± 143 (180, 534)	25 ± 12 (9, 42)
n-Butane	1472 ± 407 (817, 2123)	137 ± 94 (38, 317)	649 ± 312 (355, 1098)	45 ± 21 (8, 80)	1568 ± 728 (375, 2587)	4 ± 2 (ND, 7)	756 ± 355 (372, 1354)	41 ± 20 (18, 63)
i-Pentane	1130 ± 287 (572, 1490)	58 ± 71 (9, 226)	753 ± 386 (320, 1408)	23 ± 13 (ND, 39)	1952 ± 910 (502, 3189)	ND (ND, 6)	836 ± 371 (307, 1554)	24 ± 15 (9, 50)
n-Pentane	462 ± 153 (246, 709)	32 ± 28 (7, 89)	301 ± 154 (147, 549)	13 ± 7 (ND, 23)	785 ± 374 (175, 1253)	ND (ND, ND)	295 ± 132 (121, 524)	12 ± 7 (5, 21)
Ethene	891 ± 303 (453, 1281)	36 ± 40 (9, 128)	937 ± 559 (368, 1754)	27 ± 13 (11, 49)	1765 ± 1030 (414, 3391)	7 ± 2 (3, 10)	750 ± 283 (254, 1215)	21 ± 10 (9, 36)
Propene	156 ± 75 (50, 282)	6 ± 4 (3, 14)	187 ± 97 (75, 310)	13 ± 7 (ND, 22)	260 ± 161 (50, 510)	ND (ND, ND)	132 ± 59 (44, 233)	4 ± 5 (ND, 16)
Ethyne	1283 ± 238 (1007, 1652)	344 ± 62 (252, 443)	1193 ± 553 (626, 1956)	212 ± 56 (119, 304)	2102 ± 1148 (677, 3972)	28 ± 13 (17, 60)	888 ± 258 (479, 1285)	135 ± 40 (86, 212)
Benzene	292 ± 54 (230, 384)	91 ± 24 (67, 135)	260 ± 90 (151, 409)	46 ± 15 (21, 70)	437 ± 202 (140, 774)	7 ± 3 (ND, 10)	207 ± 48 (117, 268)	38 ± 14 (24, 66)
Toluene	699 ± 231 (360, 1078)	29 ± 40 (4, 122)	844 ± 382 (425, 1533)	28 ± 21 (11, 79)	1345 ± 738 (320, 2468)	8 ± 5 (ND, 15)	567 ± 226 (217, 922)	20 ± 6 (13, 31)
Ethylbenzene	97 ± 33 (51, 139)	ND (ND, 12)	100 ± 66 (20, 198)	ND (ND, 6)	85 ± 37 (37, 157)	ND (ND, 4)	196 ± 115 (43, 392)	ND (ND, ND)

There is considerable diurnal variation in the mixed layer height of the Los Angeles basin (Lu and Turco, 1995, 1996). During the nighttime the mixed layer is close to the ground, and below the height of the Mt. Wilson Observatory, but daytime upslope winds and heated mountain slopes vent air masses up the sides of the basin to reach above the height of the Observatory. The CO and hydrocarbon mixing ratio maxima are observed when upslope venting is active and the sampling site is exposed to emissions from the Los Angeles urban area. Conversely, during the evening the mountain slopes cool, preventing upslope venting and causing the top of the mixed layer to contract below the level of the Observatory, thus leading to nighttime minima of CO and hydrocarbon mixing ratios.

Only the samples from Thursday, February 14th, show almost no diurnal variation in mixing ratios for CO (Fig. 2) and the hydrocarbons (not shown). Temperatures remained below 1 °C for the entire day/night period, the lowest measured during any of the field seasons. Lower temperatures decrease the efficiency of upslope venting; however, it remains uncertain whether the low temperatures alone, or additional meteorological factors, contributed to the absence of daytime hydrocarbon and CO mixing ratio maxima. Based on the pattern of daytime maxima and nighttime minima mixing ratios observed during all other days during this campaign, it is assumed that Mt. Wilson remained above the influence of the boundary layer for the entirety of February 14th. Therefore, the February 14th measurements were considered to be non-representative of air coming from the Los Angeles basin and are excluded from further analysis.

The lowest background mixing ratios for CO and the hydrocarbons were observed in September, dropping below the 3 pptv limit of detection on at least one occasion for i-butane, n-butane, i-pentane, n-pentane, propene, benzene, toluene, and ethylbenzene. Diminished background mixing ratios are expected during the late summer as a consequence of strong solar intensity and correspondingly shorter photochemical lifetimes (Finlayson-Pitts and Pitts, 2000). When compared to remote background seasonal CO averages for this latitude band (Lopez, 2002; Novelli and Masarie, 2009), the amplitude of the seasonal variation in the nighttime mixing ratios at the Mt. Wilson Observatory was comparable (Table 1). The low background CO levels measured during the night at Mt. Wilson support a conclusion that the sampling site was influenced by fresh pollution during the daytime only and was representative of the background troposphere at night.

Not only did the September sampling period exhibit the lowest observed nighttime mixing ratios of CO and hydrocarbons in this study, but it also exhibited the highest (with the exception of ethylbenzene) and most variable daytime maxima (Table 1), thus resulting in the most extreme diurnal variability. Temperatures during the September period were significantly higher, with an average daytime (10:00–18:00 local time) temperature of 22 °C (±3), compared to 14 °C (±6), 15 °C (±4), and 10 °C (±5), respectively for the April/May, November, and February periods. However, daytime wind speeds were relatively low and coming from the SE for the majority of the September sampling, with only a minor episode of winds from the WNW (Fig. 3). High temperatures increase evaporative rates, which could lead to elevated hydrocarbon mixing ratios, especially from stored fuel and solvents. However, high temperatures also inflate boundary layer heights, which could increase upslope mixing but also dilution processes, so may decrease the observed hydrocarbon mixing ratios. Additionally, low winds tend to allow the air mass to accumulate emissions over a longer period of time. Other meteorological factors that could have contributed to the results observed during September are increased solar radiation and decreased relative humidity, which could influence photochemical processing.

To better understand the different influences on hydrocarbon mixing ratios and to explain the high daytime hydrocarbon mixing ratios observed during September, we look at ratios of the different components with CO. Carbon monoxide, a product of incomplete combustion, is an excellent tracer of combustion processes in urban areas (Parrish, 2006; Baker et al., 2008). To account for variations in dilution due to mixed layer height, the daytime (10:00–18:00 local time) hydrocarbon mixing ratios were normalized to CO (Table 2). The nonmethane hydrocarbons generally correlate well with CO (R^2 values generally greater than 0.7), which suggests that they originate from similar or co-located sources. However, the correlations were strongest during April/May and September with typical R^2 values greater than 0.8. During February and November, R^2 values fell below 0.7 for propane and propene, and for ethane during February. This could be attributed to higher temperatures and better mixing during the April/May and September sampling periods.

Based on estimates from the California Air Resources Board, mobile sources (primarily on-road motor vehicles) dominate CO emissions at 3247 metric tonnes of CO per day, which corresponds to approximately 92% of total CO emissions in the South Coast air basin (CARB, 2007b). The C_5 alkanes, alkenes, ethyne, and aromatics are typically associated with transport related emissions (Baker et al., 2008), therefore strong correlations with CO are consistent with fresh automobile combustion. Conversely, C_2–C_4 alkanes are not strongly associated with vehicular emissions (Baker et al., 2008), so their relatively strong correlation with CO at the Mt. Wilson site would suggest that the urban Los Angeles basin air mass, with its myriad of sources, is typically thoroughly mixed by the time it reaches Mt. Wilson, especially for the warmer months.

While the correlation between hydrocarbons and CO remains strong, there is considerable seasonal variation in the hydrocarbon to CO ratios (Table 2). The lowest hydrocarbon/CO ratios were typically observed during November, while September and February exhibited the highest ratios. Ethane and propane exhibit the highest hydrocarbon/CO ratios for all the seasons, whereas the lowest and least variable ratios were observed for propene, benzene, and ethylbenzene. The C_2–C_5 alkanes exhibited the greatest variability between the seasons, with n-butane varying by more than a factor of two between February and April/May. In the Los Angeles area C_2–C_5 alkanes share common sources from evaporative emissions and liquid/unburned gasoline (Brown et al., 2007), and variability in source magnitude and transport efficiency could explain the observed seasonal differences in hydrocarbon/CO ratios.

3.2. Emission estimates

The source of CO is fairly well quantified for the Los Angeles basin (Fujita et al., 2003). By contrast, speciated hydrocarbon emission inventories (EIs) are not well established, except for selected toxic compounds, and even then air quality models for Los Angeles and the South Coast Air Basin typically rely on lumped hydrocarbon emissions (M. Carreras-Sospedra, Personal Communication, 2009). In an effort to improve hydrocarbon EIs we use hydrocarbon/CO ratios to estimate hydrocarbon emissions relative to CO emission inventories, similar to the "top down" approach used by Hsu et al. (2010) to calculate methane emissions.

The California Air Resources Board (CARB) estimates annual average emissions of CO during 2006 at 3547 metric tonnes CO per day in the South Coast Air Basin (CARB, 2007b). We use this value for CO along with the annual average slope for the relationship of nonmethane hydrocarbons versus CO from our measurements to estimate annual average hydrocarbon emissions (Table 3).

Modeled emissions of benzene and toluene for the South Coast Air Basin (2005) are 10.2 and 37.6 metric tonnes per day, respectively (AQMD, 2008). These model results agree relatively well with emissions of 12 and 47 metric tonnes per day calculated for benzene and toluene, respectively, from our Mt. Wilson measurements
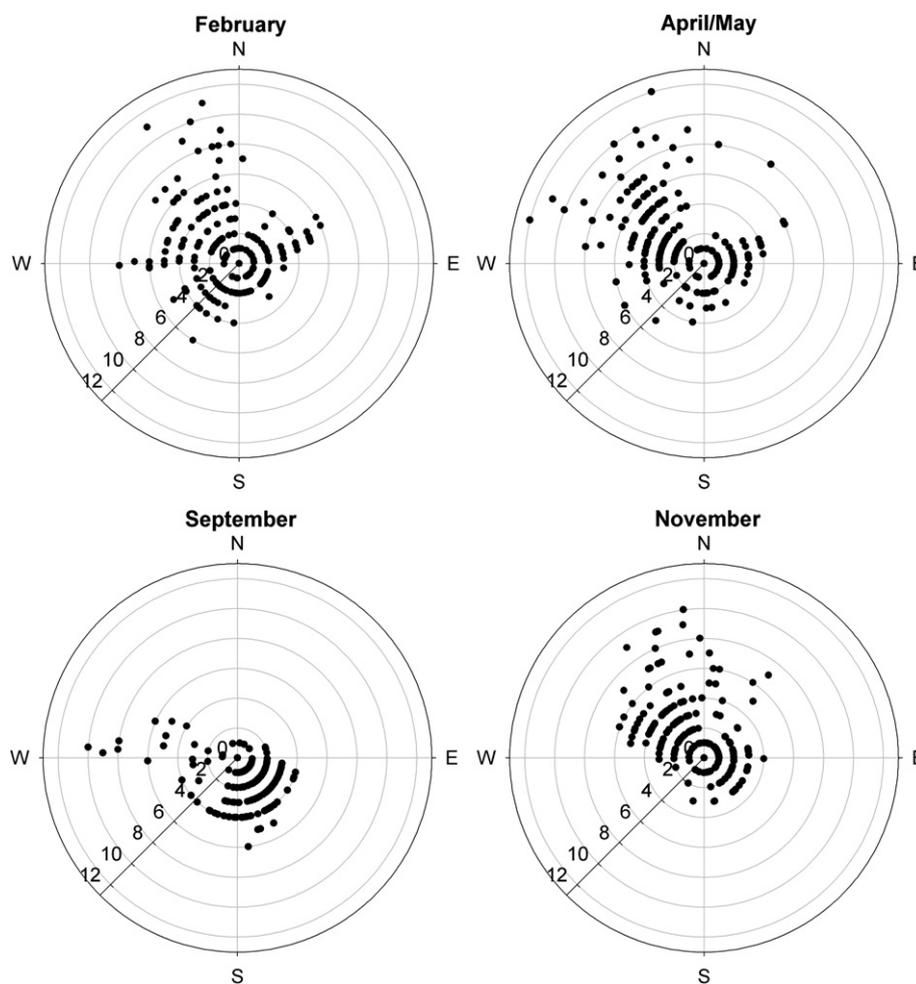
Fig. 3. Daytime (10:00–18:00 local time) wind speed and direction during four different sampling periods. Wind speed is expressed as axial units in m s^{-1} and wind direction is expressed as radial units in degrees.

(Table 3), and confirms the Mt. Wilson site as a useful location for establishing emission estimates for the Los Angeles basin.

Ethane emissions calculated here account for approximately 0.7% of the total United States emissions, which are estimated to be 2.4 Tg yr^{-1} by Xiao et al. (2008). Considering that the greater Los Angeles metropolitan area represents approximately 4.2% of the total United States population (U.S. Census Bureau, 2009), per capita ethane emissions for this region are low. Other regions, such as the Midwestern and Eastern United States where there are large

local natural gas and coal mining operations, likely have much higher per capita ethane emissions (Baker et al., 2008).

Average emissions of propane are the greatest of all measured hydrocarbons in terms of metric tonnes per day (Table 3). However, in order to assess the ozone-generating potential for any particular species both the abundance and the relative reactivity must be considered. Carter (1994) developed the maximum incremental reactivity (MIR) scale as a way of assessing the reactivity of different VOCs, where MIR is defined as grams of ozone produced per gram

Table 2
Daytime (10:00–18:00 local time) hydrocarbon to CO ratios during four different sampling periods. Quoted uncertainties are 1-sigma.

Compound	February		April/May		September		November	
	Slope	R^2	Slope	R^2	Slope	R^2	Slope	R^2
Ethane	12.47 ± 1.03	0.65	10.58 ± 0.56	0.82	13.07 ± 0.50	0.90	8.88 ± 0.45	0.83
Propane	12.54 ± 1.09	0.63	12.27 ± 0.50	0.89	13.58 ± 0.52	0.90	8.88 ± 0.67	0.69
i-Butane	3.63 ± 0.26	0.71	2.24 ± 0.09	0.89	2.77 ± 0.23	0.65	1.88 ± 0.10	0.81
n-Butane	7.82 ± 0.44	0.80	3.33 ± 0.15	0.86	3.88 ± 0.24	0.76	4.18 ± 0.28	0.74
i-Pentane	6.57 ± 0.30	0.86	4.24 ± 0.17	0.89	5.36 ± 0.18	0.92	4.54 ± 0.32	0.72
n-Pentane	2.58 ± 0.14	0.81	1.71 ± 0.06	0.90	2.11 ± 0.09	0.87	1.63 ± 0.10	0.77
Ethene	5.55 ± 0.25	0.86	5.62 ± 0.24	0.87	5.11 ± 0.14	0.94	4.08 ± 0.21	0.83
Propene	0.92 ± 0.07	0.68	0.94 ± 0.06	0.78	0.72 ± 0.03	0.88	0.62 ± 0.05	0.62
Ethyne	5.75 ± 0.22	0.89	5.61 ± 0.24	0.87	5.83 ± 0.15	0.95	4.25 ± 0.15	0.91
Benzene	1.21 ± 0.06	0.85	1.12 ± 0.05	0.88	1.20 ± 0.02	0.98	0.94 ± 0.03	0.93
Toluene	4.28 ± 0.19	0.86	4.47 ± 0.20	0.86	3.92 ± 0.16	0.88	3.01 ± 0.18	0.77
Ethylbenzene	0.64 ± 0.04	0.80	0.62 ± 0.03	0.84	0.60 ± 0.02	0.89	0.44 ± 0.03	0.73

Table 3
Estimates of annual average daily hydrocarbon emissions using estimated annual average CO emissions of 3547 metric tonnes per day. Quoted uncertainties are 1-sigma.

Hydrocarbon	R^2	HC versus CO slope	MIR[a]	HC Emission (metric tonnes per day)
Ethane	0.79	12.2 ± 0.4	0.25	46
Propane	0.81	12.8 ± 0.3	0.48	71
i-Butane	0.64	2.8 ± 0.1	1.21	21
n-Butane	0.60	4.2 ± 0.2	1.02	31
i-Pentane	0.83	5.3 ± 0.1	1.38	48
n-Pentane	0.80	2.1 ± 0.1	1.04	19
Ethene	0.89	5.2 ± 0.1	7.4	18
Propene	0.78	0.8 ± 0.0	9.4	4
Ethyne	0.90	5.6 ± 0.1	0.50	18
Benzene	0.89	1.2 ± 0.0	0.42	12
Toluene	0.86	4.0 ± 0.1	2.7	47
Ethylbenzene	0.85	0.6 ± 0.0	2.7	8

[a] Maximum incremental reactivity. Units of grams ozone formed per gram VOC emitted.

of VOC. Short-lived gases, such as the alkenes and substituted aromatics, are more reactive and have a greater potential to contribute to ozone formation (Table 3). Based on both MIR and emission estimates, for the gases reported here, ethene, toluene, and i-pentane are the greatest contributors to ozone production in the Los Angeles basin. However, the MIR estimates are based on VOC oxidation by OH, and do not account for additional ozone formation as the result of VOC oxidation by Cl, which will be discussed in the following section.

Qin et al. (2004), reported detailed results of weekend–weekday variation of speciated hydrocarbon ozone formation potentials at different sites in the Los Angeles basin. Ozone formation potentials determined from mid-day measurements (14:00, local time) made in Burbank and Azusa (both are located near Los Angeles and experience the weekend effect) exhibited the greatest potential for ethene, toluene, i-pentane, and are in good agreement with our estimates from the Mt. Wilson measurements.

3.3. Evidence of Cl atom chemistry

In polluted urban areas, chlorine (Cl) atoms originating from a marine atmosphere are thought to contribute significantly to the oxidation of organics (Finlayson-Pitts, 1993). As discussed in detail by Finlayson-Pitts (1993) coastal wave action results in the suspension of NaCl particles which react to form products (such as ClNO, ClNO$_2$, and Cl$_2$) that are photolyzed to generate Cl atoms. In the presence of Cl atoms, VOCs are oxidized to reactive alkyl radicals, which can then contribute to ozone formation similarly to OH initiated oxidation of organics. This, and the coastal proximity of the Los Angeles basin, led us to investigate evidence of alternative oxidation pathways via Cl atom chemistry during this study.

Air mass origin was evaluated using FLEXPART (Stohl et al., 2005), a high-resolution Lagrangian particle dispersion model, and atmospheric back trajectories. Calculated daily at 13:00 (local time) from September 8 to 16, three-day back trajectories indicate that air masses during the September sampling period were typically originating from coastal and oceanic regions before being sampled at Mt. Wilson (Fig. 4a). With the exception of September 10th, all of the September back trajectories show air masses transported over the coast near the Los Angeles basin with 1-day or less in travel time before being transported north or northeast to arrive at the Mt. Wilson site (Fig. 4b). Daily back trajectories calculated for the April/May sampling period also showed considerable oceanic influence, while air masses during the February and November periods typically were transported over land for two or more days prior to being sampled at Mt. Wilson.
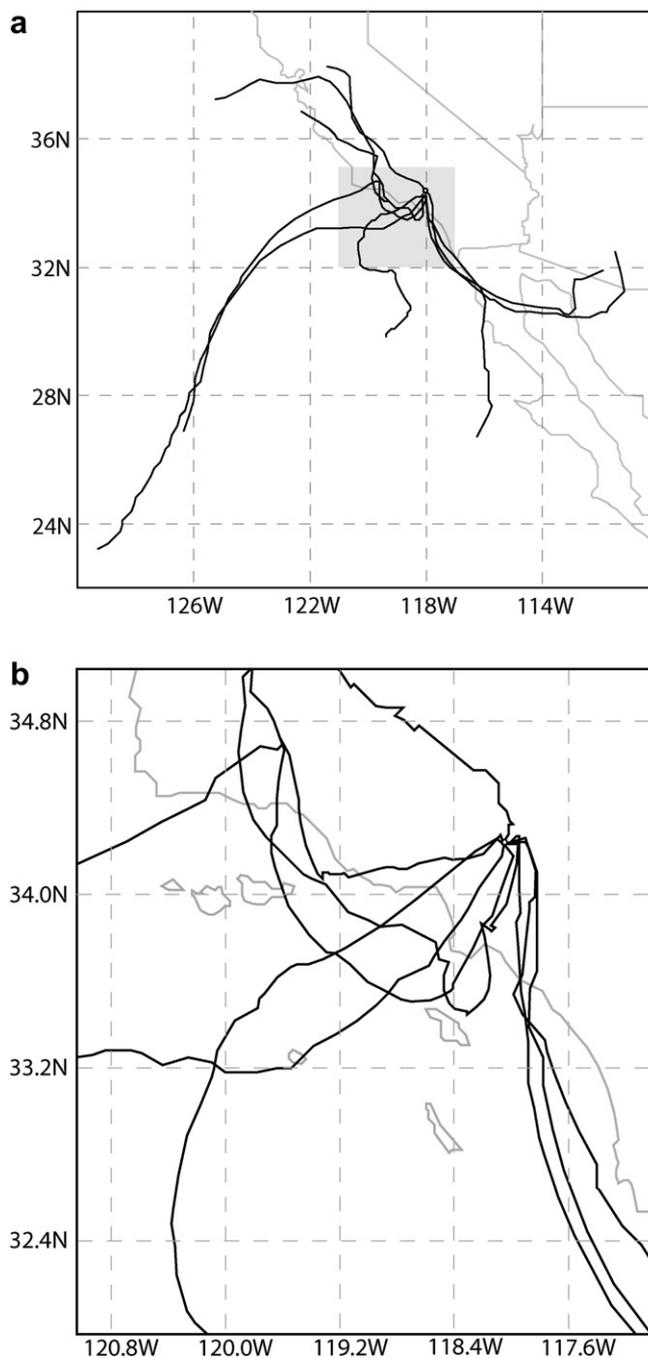

Fig. 4. Panel (a) shows three-day air mass back trajectories for Mt. Wilson calculated daily from September 8 to 16, 2007, at 13:00 (local time). Panel (b) shows close up view (shaded region in panel (a)) near the Southern California coast.

The short-lived halocarbons CHBr$_3$ and CH$_2$Br$_2$ have previously been shown to have a strong oceanic source and have been used as tracers to evaluate recent marine influence on air masses (Blake et al., 1992, 1999; Zhou et al., 2005; Butler et al., 2007). The CHBr$_3$ and CH$_2$Br$_2$ measurements during September exhibited enhanced daytime maxima mixing ratios of 3.2 ± 1.0 pptv and 1.4 ± 0.5 pptv, respectively. These enhancements are comparable to results from Zhou et al. (2005) at inland sites near Great Bay, New Hampshire, which attributed enhanced summertime mixing ratios of 4.9 pptv and 1.3 pptv for CHBr$_3$ and CH$_2$Br$_2$, respectively, to coastal influence. Daytime enhancements of CHBr$_3$ and CH$_2$Br$_2$
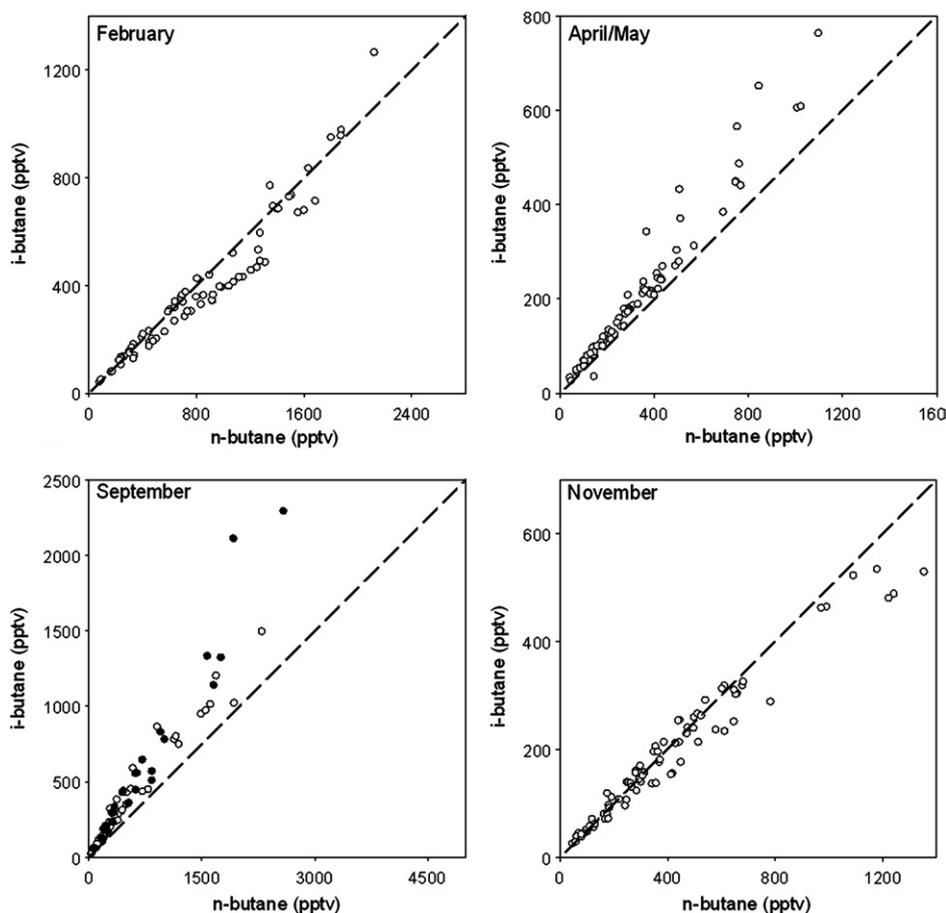
Fig. 5. Relationship between daytime (10:00–18:00 local time) *i*-butane and *n*-butane for each of the sampling periods. The slope expected from OH kinetics only is indicated by the dashed line. Samples collected during the September 12–15 period are indicated by filled circles.

were also observed during April/May periods when back trajectories indicated oceanic influence within 24-h of arriving at Mt. Wilson.

Relationships between selected hydrocarbon species can be used to probe for evidence of halogen chemistry. Both *i*-butane and *n*-butane have similar sources and, in a normal background atmosphere dominated by OH oxidation, both butanes are destroyed at approximately the same rate ($k_{OH+n\text{-butane}} = 2.36 \times 10^{-12}$ and $k_{OH+i\text{-butane}} = 2.12 \times 10^{-12}$ cm³ molecule; Atkinson, 2003). Thus, typical *i*-butane to *n*-butane tropospheric ratios are approximately 0.5 pptv pptv^{-1} (Jobson et al., 1994; Swanson et al., 2003). When Cl atom oxidation is active, the loss of *n*-butane with respect to Cl is approximately 50% faster than the loss of *i*-butane ($k_{Cl+n\text{-butane}} = 2.2 \times 10^{-10}$ and $k_{Cl+i\text{-butane}} = 1.4 \times 10^{-10}$ cm³ molecules^{-1} s^{-1}; Atkinson, 1997), which results in a perturbation of the *i*-butane to *n*-butane ratio. As discussed in detail by Jobson et al. (1994), Br atom reacts more than six orders of magnitude slower with the butanes than Cl, therefore Br atom has a negligible impact on the *i*-butane to *n*-butane ratio.

The mean daytime *i*-butane to *n*-butane ratio (± 1-SD) was calculated for each of the different sampling periods. Daytime values of 0.47 (± 0.06), 0.61 (± 0.08), 0.75 (± 0.13), and 0.49 (± 0.07), were obtained for February, April/May, September, and November, respectively (Fig. 5). The ratio for September exhibited the greatest daytime variability (minimum of 0.53 and maximum of 1.11) and deviation from the expected 0.5 value. Within this sampling period, the time from 12:00 (local time) September 12 to 12:00 (local time) September 15 (2007) had a particularly elevated daytime *i*-butane/

n-butane ratio of 0.82 (± 0.12) and $R^2 = 0.95$ (Fig. 5), suggesting the presence of increased Cl activity during this time.

Assuming that the observed *n*-butane depletion is caused by Cl oxidation, Cl concentrations can be estimated based on reaction kinetics (Jobson et al., 1994),

$$[n\text{-butane}]_{low} = [n\text{-butane}]_{background} \exp(-k_{Cl} \int [Cl] \, dt)$$

where $[n\text{-butane}]_{low}$ is the average daytime maxima *n*-butane mixing ratio during September (Table 1), $[n\text{-butane}]_{background}$ is twice the average daytime maxima *i*-butane mixing ratio during September (Table 1), k_{Cl} is the Cl atom rate constant for reaction with *n*-butane, and d*t* is the estimated processing time. When a 1-day processing time is assigned, Cl is calculated to be 3.1×10^4 atom cm^{-3}. Applying this approach to the high *i*-butane/*n*-butane ratios observed during the September 12–15 time period resulted in a maximum Cl concentration of 6.5×10^4 atom cm^{-3}. This Cl concentration is comparable to estimates of 10^4 atom cm^{-3} made by Arsene et al. (2007) for a marine site in the Eastern Mediterranean. The 1-day processing time used here is based on estimated FLEXPART back trajectory transport times during September. Some back trajectories during September showed transport from the coast to Mt. Wilson in less than 1-day, in which case this would likely underestimate Cl concentrations.

One of the uncertainties of using hydrocarbons as indicators of halogen activity is whether the enhanced *i*-butane/*n*-butane ratios are a result of Cl oxidation or mixing of air masses with different photochemical ages. Previous studies used the kinetic relationship between
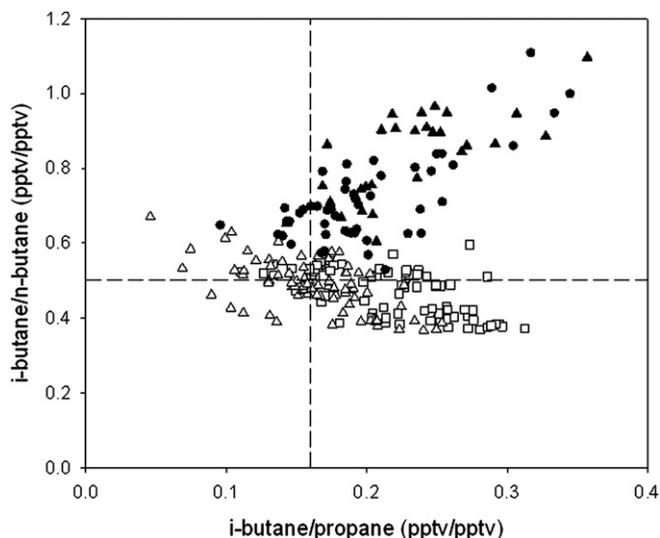
Fig. 6. Daytime (10:00–18:00 local time) *i*-butane/*n*-butane versus *i*-butane/propane for September (filled circle), November (open triangle), and February (open square). Samples collected during September 12–15 period are indicated by filled triangle. Dashed lines indicate approximately how data would align under OH kinetics (horizontal) and Cl kinetics (vertical).

different hydrocarbon ratios to deduce whether oxidation is occurring primarily via OH or Cl (e.g. Parrish et al., 1993; Jobson et al., 1994; Arsene et al., 2007). As discussed in detail by Parrish et al. (1993), OH and Cl oxidation can be clearly distinguished from each other by plotting *i*-butane/*n*-butane versus *i*-butane/propane. For OH kinetics the *i*-butane/*n*-butane will remain constant while *i*-butane/propane will decrease with processing time. Conversely, for Cl kinetics the *i*-butane/propane will remain constant and the *i*-butane/*n*-butane will increase with processing time. Additionally, by including propane in this analysis the atmospheric dilution effect is diminished. Shown in Fig. 6 is *i*-butane/*n*-butane versus *i*-butane/propane for September compared with November and February. The November and February results follow the horizontal axis and are indicative of OH kinetics, while the September results fall between the horizontal and the vertical axis suggesting that there is a mix of OH and Cl kinetics. The April/May results (not shown) exhibited scatter between OH and Cl kinetics. The behavior of hydrocarbon ratios is a valuable tool to indirectly evaluate the presence of Cl atoms, however, it should be noted that it does not completely rule out other processes.

Though OH is generally the dominant atmospheric oxidant, the reaction of Cl with alkanes is typically two orders of magnitude faster than with OH (Finlayson-Pitts, 1993). Typical tropospheric OH concentrations are 10^5–10^7 molecules cm^{-3} (Spivakovsky et al., 2000), therefore when Cl concentrations are on the order of 10^4 molecules cm^{-3} the destruction of hydrocarbons by OH and Cl is comparable. Oxidation of VOCs by Cl is expected to increase ozone formation potentials, and as discussed by Cohan et al. (2008), the inclusion of Cl chemistry in air quality models for the Los Angeles area resulted in enhanced ozone levels.

These results suggest that oceanic influence, as seen from air mass back trajectories and halocarbon tracers, was responsible for enhanced Cl activity during our September study period. Because Cl reacts very quickly with a range of hydrocarbon species, concentrations of the magnitude estimated here could have considerable impact on ozone formation within the Los Angeles basin.

4. Conclusions

Measurements at Mt. Wilson of air masses coming from the Los Angeles basin show considerable differences in nonmethane

hydrocarbons diurnally as well as between seasons. Using measured hydrocarbon to CO ratios, annual average hydrocarbon emissions from the South Coast air basin were estimated. Differences in non-methane hydrocarbon mixing ratios appear to relate to seasonal variations in meteorological parameters such as wind speed, wind direction, temperature, and air mass origin. Measurements made during September exhibited elevated hydrocarbon mixing ratios as well as changes in the hydrocarbon to CO relationship, when compared to the other seasons. Additionally, indirect evidence of Cl atom chemistry and oceanic influence was observed at the Mt. Wilson site during the September campaign.

Mt. Wilson served as an excellent location for monitoring pollution originating from the Los Angeles basin, and has the potential to become a valuable monitoring station. The site offered several advantages as a representative sampling location for the Los Angles basin, including exposure to well mixed air masses coming from the basin, and distinct diurnal variations where both polluted and free troposphere background air masses could be sampled. The results of this study illustrate the importance of considering hydrocarbons from a seasonal perspective in order to fully account for changes in the hydrocarbon mixing ratios and source character, as well as influences from variable meteorological conditions.

References

AAPA, 2008. Port Industry Statistics. American Association of Port Authorities. <www.aapa-ports.org/Industry/content.cfm?ItemNumber=900>.

AQMD, 2008. MATES III Final Report. South Coast Air Quality Management District, Diamond Bar, CA. <http://www.aqmd.gov/prdas/matesIII/matesIII.html>.

Arsene, C., Bougiatioti, A., Kanakidou, M., Bonsang, B., Mihalopoulos, N., 2007. Tropospheric OH and Cl levels deduced from non-methane hydrocarbon measurements in a marine site. Atmospheric Chemistry and Physics 7, 4661–4673.

Atkinson, R., 1997. Gas-phase tropospheric chemistry of volatile organic compounds: 1. Alkanes and alkenes. Journal of Physical and Chemical Reference Data 26, 215–290.

Atkinson, R., 2003. Kinetics of the gas-phase reactions of OH radicals with alkanes and cycloalkanes. Atmospheric Chemistry and Physics 3, 2233–2307.

Baker, A.K., Beyersdorf, A.J., Doezema, L.A., Katzenstein, A., Meinardi, S., Simpson, I.J., Blake, D.R., Rowland, F.S., 2008. Measurements of nonmethane hydrocarbons in 28 United States cities. Atmospheric Environment 42, 170–182.

Blake, D.R., Blake, N.J., Smith, T.W., Wingenter, O.W., Rowland, F.S., 1996. Non-methane hydrocarbon and halocarbon distributions during Atlantic Stratocumulus Transition Experiment/Marine Aerosol and Gas Exchange, June 1992. Journal of Geophysical Research 101, 4501–4514.

Blake, N.J., Blake, D.R., Wingenter, O.W., Sive, B.C., Kang, C.H., Thornton, D.C., Bandy, A.R., Atlas, E., Blocke, F., Harris, J.M., Rowland, F.S., 1999. Aircraft measurements of the latitudinal, vertical, and seasonal variations of NMHCs, methyl nitrate, methyl halides, and DMS during the First Aerosol Characterization Experiment (ACE 1). Journal of Geophysical Research 104, 21803–21817.

Brown, S.G., Frankel, A., Hafner, H.R., 2007. Source apportionment of VOCs in the Los Angeles area using positive matrix factorization. Atmospheric Environment 41, 227–237.

Butler, J.H., King, D.B., Lobert, J.M., Montzka, S.A., Yvon-Lewis, S.A., Hall, B.D., Warwick, N.J., Mondeel, D.J., Aydin, M., Elkins, J.W., 2007. Oceanic distributions and emissions of short-lived halocarbons. Global Biogeochemical Cycles 21. doi:10.1029/2006GB002732.

CARB, 2007a. Air Quality Data Area Designations, 2007. California Air Resources Board, Sacramento, CA. <http://www.arb.ca.gov/desig/desig.htm>.

CARB, 2007b. Estimated Annual Emissions for South Coast Air Basin, 2006. California Air Resources Board, Sacramento, CA. <http://www.arb.ca.gov/ei/ei.htm>.

Carreras-Sospedra, M., 2009. Personal Communication. University of California, Irvine.

Carter, W.P.L., 1994. Development of ozone reactivity scales for volatile organic compounds. Journal of the Air and Waste Management Association 44, 881–899.

Chameides, W.L., Fehsenfeld, F., Rodgers, M.O., Cardelino, C., Martinez, J., Parrish, D., Lonneman, W., Lawson, D.R., Rasmussen, R.A., Zimmerman, P., Greenberg, J., Middleton, P., Wang, T., 1992. Ozone precursor relationships in the ambient atmosphere. Journal of Geophysical Research 97, 6037–6055.

Chung, M.Y., Maris, C., Krischke, U., Meller, R., Paulson, S.E., 2003. An investigation of the relationship between total non-methane organic carbon and the sum of speciated hydrocarbons and carbonyls measured by standard GC/FID: measurements in the Los Angeles air basin. Atmospheric Environment 37, S159–S170.

Cohan, A., Chang, W., Carreras-Sospedra, M., Dabdub, D., 2008. Influence of sea-salt activated chlorine and surface-mediated renoxification on the weekend effect in the South Coast Air Basin in California. Atmospheric Environment 42, 3115–3129.

Colman, J.J., Swanson, A.L., Meinardi, S., Sive, B.C., Blake, D.R., Rowland, F.S., 2001. Description of the analysis of a wide range of volatile organic compounds in whole air samples collected during PEM-tropics A and B. Analytical Chemistry 73, 3723–3732.

Croes, B.E., Fujita, E.M., 2003. Overview of the 1997 Southern California ozone study (SCOS97-NARSTO). Atmospheric Environment 37, S3–S26.

Elkus, B., Wilson, K.R., 1977. Photochemical air pollution: weekend–weekday differences. Atmospheric Environment 11, 509–515.

Finlayson-Pitts, B.J., 1993. Chlorine atoms as a potential tropospheric oxidant in the marine boundary layer. Research on Chemical Intermediates 19, 235–249.

Finlayson-Pitts, B.J., Pitts, J.N., 2000. Chemistry of the Upper and Lower Atmosphere. Academic Press, San Diego.

Fraser, M.P., Cass, G.R., Simoneit, B.R.T., Rasmussen, R.A., 1997. Air quality model evaluation data for organics. 4. C_2–C_{36} non-aromatic hydrocarbons. Environmental Science and Technology 31, 2356–2367.

Fujita, E.M., Campbell, D.E., Zielinska, B., Sagebiel, J.C., Bowen, J.L., Goliff, W.S., Stockwell, W.R., Lawson, D.R., 2003. Diurnal and weekday variations in the source contributions of ozone precursors in California's South Coast air basin. Journal of the Air and Waste Management Association 53, 844–863.

Gordon, R.J., Mayrsohn, H., Ingels, R.M., 1968. C_2–C_5 hydrocarbons in the Los Angeles atmosphere. Environmental Science and Technology 2, 1117–1120.

Haagen-Smit, A.J., 1952. Chemistry and physiology of Los Angeles smog. Industrial and Engineering Chemistry 44, 1342–1346.

Hsu, Y.-K., VanCuren, T., Park, S., Jakober, C., Herner, J., Fitzgibbon, M., Blake, D.R., Parrish, D.D., 2010. Methane emissions inventory verification in Southern California. Atmospheric Environment 44, 1–7.

Jobson, B.T., Niki, H., Yokouchi, Y., Bottenheim, J., Hopper, F., Leaitch, R., 1994. Measurements of C_2–C_6 hydrocarbons during the polar sunrise 1992 experiment: evidence for Cl atom and Br atom Chemistry. Journal of Geophysical Research 99, 25355–25368.

Levitt, S.B., Chock, D.P., 1976. Weekday–weekend pollutant studies of the Los Angeles basin. Journal of the Air Pollution Control Association 26, 1091–1092.

Lippmann, M., 1991. Health effects of tropospheric ozone. Environmental Science and Technology 25, 1954–1962.

Lopez, J.D.P., 2002. Seasonality and Global Trends of Carbon Monoxide During 1995–2001. Dissertation, University of California, Irvine.

Lu, R., Turco, R.P., 1995. Air pollutant transport in a coastal environment – II. Three-dimensional simulations over Los Angeles basin. Atmospheric Environment 29, 1499–1518.

Lu, R., Turco, R.P., 1996. Ozone distributions over the Los Angeles basin: three-dimensional simulations with the smog model. Atmospheric Environment 30, 4155–4176.

Lonneman, W.A., Kopczynski, S.L., Darley, P.E., Sutterfield, F.D., 1974. Hydrocarbon composition of urban air pollution. Environmental Science and Technology 8, 229–236.

Novelli, P.C., Masarie, K.A., 2009. Atmospheric Carbon Monoxide Dry Air Mole Fractions from the NOAA ESRL Carbon Cycle Cooperative Global Air Sampling Network, 1998–2008. Version: 2009-07-28. <ftp://ftp.cmdl.noaa.gov/ccg/co/flask/event>.

Parrish, D.D., Hahn, C.J., Williams, E.J., Norton, R.B., Fehsenfeld, F.C., Singh, H.B., Shetter, J.D., Gandrud, B.W., Ridley, B.A., 1993. Reply. Journal of Geophysical Research 98, 14995–14997.

Parrish, D.D., 2006. Critical evaluation of US on-road vehicle emission inventories. Atmospheric Environment 40, 2288–2300.

Qin, Y., Tonnesen, G.S., Wang, Z., 2004. Weekend/weekday differences of ozone, NO_x, CO, VOCs, PM_{10} and the light scatter during ozone season in Southern California. Atmospheric Environment 38, 3069–3087.

Renzetti, N.A., 1956. Ozone in the Los Angeles atmosphere. Journal of Chemical Physics 24, 909.

Spivakovsky, C.M., Logan, J.A., Montzka, S.A., Balkanski, Y.J., Foreman-Fowler, M., Jones, D.B.A., Horowitz, L.W., Fusco, A.C., Brenninkmeijer, C.A.M., Prather, M.J., Wofsy, S.C., McElroy, M.B., 2000. Three-dimensional climatological distribution of tropospheric OH: update and evaluation. Journal of Geophysical Research 105, 8931–8980.

Stohl, A., Forster, C., Frank, A., Seibert, P., Wotawa, G., 2005. Technical note: the Lagrangian particle dispersion model FLEXPART version 6.2. Atmospheric Chemistry and Physics 5, 2461–2474.

Swanson, A.L., Blake, N.J., Atlas, E., Flocke, F., Blake, D.R., Rowland, F.S., 2003. Seasonal variations of C_2–C_4 nonmethane hydrocarbons and C_1 C_4 alkyl nitrates at the Summit research station in Greenland. Journal of Geophysical Research 108, 4065–4073.

U.S. Census Bureau, 2009. United States Census, 2007. United States Department of Commerce. <http://www.census.gov>.

Xiao, Y., Logan, J.A., Jacob, D.J., Hudman, R.C., Yantosca, R., Blake, D.R., 2008. Global budget of ethane and regional constraints on U.S. sources. Journal of Geophysical Research 113. doi:10.1029/2007JD009415.

Zhou, Y., Varner, R.K., Russo, R.S., Wingenter, O.W., Haase, K.B., Talbot, R., Sive, B.C., 2005. Coastal water source of short-lived halocarbons in New England. Journal of Geophysical Research 110. doi:10.1029/2004JD005603.